Journal of Computational Physics **165,** 216–236 (2000)
doi:10.1006/jcph.2000.6612, available online at http://www.idealibrary.com on IDEAL®

Fast Spectral Methods for the Fokker–Planck–Landau Collision Operator[1]

L. Pareschi,* G. Russo,† and G. Toscani‡

*Department of Mathematics, University of Ferrara, via Machiavelli 35, I-44100 Ferrara, Italy; †Department of Mathematics, University of L'Aquila, via Vetoio, loc. Coppito, I-67010 L'Aquila, Italy; and ‡Department of Mathematics, University of Pavia, via Ferrata 1, I-27100 Pavia, Italy
E-mail: pareschi@dm.unife.it, russo@univaq.it, toscani@dimat.unipv.it

Received October 14, 1999; revised June 16, 2000; published online November 3, 2000

In this paper we present a new spectral method for the fast evaluation of the Fokker–Planck–Landau (FPL) collision operator. The method allows us to obtain spectrally accurate numerical solutions with simply $O(n \log_2 n)$ operations in contrast with the usual $O(n^2)$ cost of a deterministic scheme. We show that the method preserves the total mass whereas momentum and energy are approximated with spectral accuracy. Numerical results for the FPL equation for Maxwell molecules and for Coulomb interactions in two and three dimensions in velocity space are also given. © 2000 Academic Press

Key Words: Fokker–Planck–Landau equation; spectral methods; fast Fourier transform.

1. INTRODUCTION

This paper is devoted to the development of numerical schemes for the accurate computation of the solution of the Fokker–Planck–Landau (FPL) equation. Here we will mainly concentrate on the approximation of the collision operator, and hence of the velocity space.

The FPL equation is a common kinetic model in plasma physics. It is described by a nonlinear partial integrodifferential equation

$$\frac{\partial f}{\partial t} + v \cdot \nabla_x f = Q_L(f, f), \quad x, v \in \mathbb{R}^3, \tag{1.1}$$

[1] This work was partially supported by TMR project "Asymptotic Methods in Kinetic Theory," Contract Number ERB FMRX CT97 0157.

0021-9991/00 $35.00
Copyright © 2000 by Academic Press
All rights of reproduction in any form reserved.

where Q_L is the Landau collision operator

$$Q_L(f, f)(v) = \nabla_v \cdot \int A(v - v_*)(f(v_*)\nabla_v f(v) - f(v)\nabla_{v_*} f(v_*))\, dv_*. \tag{1.2}$$

The unknown function $f = f(x, v, t)$, which represents the density of a gas in the phase space of all positions x and velocities v of particles, is assumed to be nonnegative and integrable together with its moments up to the order two.

In (1.2) A depends on the interaction between particles and is a $d \times d$ nonnegative and symmetric matrix of the form

$$A(z) = \Psi(|z|)\Pi(z). \tag{1.3}$$

Here Ψ is a nonnegative function and $\Pi(z)$ is the orthogonal projection upon the space orthogonal to z,

$$\Pi_{ij}(z) = \left(\delta_{ij} - \frac{z_i z_j}{|z|^2}\right). \tag{1.4}$$

In the case of inverse-power laws with $\gamma \geq -3$,

$$\Psi(z) = \Lambda |z|^{\gamma+2}, \tag{1.5}$$

where $\Lambda > 0$ is a constant.

As for the Boltzmann equation, different values of γ lead to the usual classification in hard potentials ($\gamma > 0$), Maxwellian molecules ($\gamma = 0$), or soft potentials ($\gamma < 0$). This latter case involves the Coulombian case $\gamma = -3$, which is of primary importance for plasma applications.

Equation (1.1) is obtained as a limit of the Boltzmann equation when all the collisions become grazing. The original derivation of the equation is due to Landau [18].

For the formal mathematical derivation of the equation, we cite Arsen'ev and Buryak [1], Degond and Lucquin-Desreux [10] and Desvillettes [12]. Recently Villani [33] obtained a complete rigorous proof of this asymptotic problem in the space homogeneous situation. The mathematical properties of the spatially homogeneous FPL equation when $\gamma > 0$ have been recently studied by Desvillettes and Villani [13].

The numerical solution of nonlinear kinetic equations, such as the FPL equation, represents a real challenge for numerical methods. This is essentially due to the nonlinearity, to the large number of variables (seven for the full problem), and to the threefold integral (1.2). In addition, this integration has to be handled carefully since it is at the basis of the macroscopic properties of the equation.

The structure of the FPL collision operator is similar to that of Boltzmann's collision operator and has the same fundamental properties of conserving mass, momentum, and energy,

$$\int_{\mathbb{R}^3} Q_L(f, f) \begin{pmatrix} 1 \\ v \\ |v|^2 \end{pmatrix} dv = 0, \tag{1.6}$$

and of satisfying the entropy inequality (H-theorem)

$$\int_{\mathbb{R}^3} Q(f, f) \log(f)\, dv \le 0. \tag{1.7}$$

The H-theorem implies that any equilibrium distribution function, i.e., any function f for which $Q_L(f, f) = 0$, has the form of a locally Maxwellian distribution

$$M(\rho, u, T)(v) = \frac{\rho}{(2\pi T)^{3/2}} \exp\left(-\frac{|u - v|^2}{2T}\right), \tag{1.8}$$

where ρ, u, and T are the density, mean velocity, and temperature of the gas given by

$$\rho = \int_{\mathbb{R}^3} f(v)\, dv, \quad u = \frac{1}{\rho} \int_{\mathbb{R}^3} v f(v)\, dv, \quad T = \frac{1}{3\rho} \int_{\mathbb{R}^3} |u - v|^2 f(v)\, dv. \tag{1.9}$$

There are several papers that refer to the numerical solution of the Fokker–Planck or the Landau–Fokker–Planck equation. Among these we recall [2, 3, 5–7, 9–11, 14, 15, 19–21, 30, 34].

Most of them are devoted to the Fokker–Planck equation [9, 20], or they consider conservative and entropic schemes in simplified situations, such as FPL equation in dimension two of velocity or spherically symmetric solutions in space homogeneous situations [2, 3, 6, 15, 30]. Entropic schemes are physically relevant and, as observed in [6], are able to prevent oscillations. The construction of a conservative and entropic scheme for the general situation has been considered by Degond and Lucquin-Desreux [11, 21] and Buet and Cordier [5]. Several fast approximated algorithms to reduce the computational complexity of these methods have been proposed recently [7, 19].

Although these fast schemes are able to preserve the most relevant physical properties, the degree of accuracy of such approaches is not clear. However, even if conservation properties are not imposed from the beginning, an accurate scheme would provide an accurate approximation of the conserved quantities. A detailed comparison of the present scheme with the schemes proposed in [7, 19] is the subject of a work in preparation [16].

Here we will extend to the FPL equation a new spectral method for the numerical solution of the homogeneous Boltzmann equation based on a Fourier spectral approximation of the collision operator (1.2) recently introduced in [25, 26]. In these papers a discretization of the collision operator based on Fourier expansion of the distribution function with respect to the velocity variable has been developed. The main advantage of the method is that we can obtain highly accurate numerical solutions at a reduced computational cost.

For the FPL equation, we show that the method reduces the quadratic cost from $O(n^2)$ to $O(n \log_2 n)$, where n is the number of parameters which characterize the discretized distribution function with respect to the velocity variable (for example, for a finite difference method with a grid in velocity space with N grid points per direction, $n = N^3$; for a Monte Carlo method where the distribution function is approximated by N particles, $n = 3N$; and so on). Furthermore, the method can be designed to preserve mass and to approximate momentum and energy with spectral accuracy; i.e., the error decreases faster than any power of the step size of the mesh in velocity [8, 17].

It is interesting to remark that, by a direct comparison of the results both in the Boltzmann and in the FPL case, one is driven to the conclusion that the spectral method gives the same problem to be solved, in which the characteristics of the collision operator are entirely

contained in the coefficients of the scheme. In other words, any bilinear integrodifferential equation of kinetic type, conserving mass, momentum, and energy, has the same spectral form. This allows us to concentrate on a high resolution of the kernel modes and to consider the development of spectral methods for the FPL grazing collision limit of the Boltzmann equation [29].

In the Boltzmann case, for the variable hard-sphere (VHS) model, the computation of such modes reduces to a single integration that in some cases (hard spheres, Maxwell molecules) can be computed explicitly. For the FPL equation, we are in a similar situation. The calculation of the kernel modes of the FPL operator requires only the computation of one-dimensional integrals for the FPL equation with two dimensions in velocity or two-dimensional integrals for the FPL equation with three dimensions in velocity (see Appendix).

The rest of the paper is organized as follows. In the next section we introduce the Fourier spectral method for the FPL equation and discuss the main properties of the scheme. Section 3 is devoted to the development of a fast algorithm for the computation of the scheme. We show how the use of transform methods allows us to reduce the cost from $O(n^2)$ to $O(n \log_2 n)$. Numerical results, for both the Maxwellian and the Coulombian case, that confirm the spectral accuracy and the efficiency of the method are given in Section 4. Finally in Section 5 we discuss some future developments. In a separate Appendix we give the details of the computation of the kernel modes.

2. SPECTRAL PROJECTION OF THE FPL EQUATION

A standard approach to the numerical solution of kinetic equations such as Eq. (1.1) is based on a splitting method (also referred to as a fractional step method). If we want to solve the equation of a time step Δt, the method consists of solving a sequence of two steps,

$$\begin{aligned} \frac{\partial \tilde{f}}{\partial t} &= Q_L(f, f), \\ \tilde{f}(x, v, 0) &= f_0(x, v), \end{aligned} \qquad \text{(collision step)}$$

$$\begin{aligned} \frac{\partial \bar{f}}{\partial t} + v \cdot \nabla_x \bar{f} &= 0, \\ \bar{f}(x, v, 0) &= \tilde{f}(x, v, \Delta t), \end{aligned} \qquad \text{(convection step)}$$

where $f_0(x, v)$ is the initial condition.

Such a scheme is only first-order accurate in time; i.e., the difference between the exact and approximate solution after one time step (local truncation error) is second order in Δt,

$$f(v, \Delta t) - \bar{f}(v, \Delta t) = O(\Delta t^2).$$

A different splitting strategy leads to a higher order approximation in time. A very common and simple scheme is Strang splitting [32], which gives second order in time. This approach has been used for the numerical solution of the Boltzmann equation in [23].

From now on we restrict ourselves to consider a spectral projection of the space homogeneous FPL equation

$$\frac{\partial f}{\partial t} = Q_L(f, f), \tag{2.10}$$

supplemented with the initial condition

$$f(v, t = 0) = f_0(v). \tag{2.11}$$

First, we observe that a simple change of variable into the FPL collision operator (1.2) permits us to write

$$Q_L(f, f)(v) = \nabla_v \cdot \int A(g)(f(v+g)\nabla_v f(v) - f(v)\nabla_g f(v+g))\, dg, \tag{2.12}$$

where $g = v - v_*$.

2.1. *Derivation of the Method*

Similarly to the Boltzmann case [25] it can be shown that for a collision operator such as (2.12) we have the following property:

PROPOSITION 2.1. *Let* $\mathrm{Supp}(f(v)) \subset \mathcal{B}(0, R)$, *where* $\mathcal{B}(0, R)$ *is the ball of radius* R *centered in the origin. Then*

$$Q_L(f, f)(v) = \nabla \cdot \int_{\mathcal{B}(0,2R)} A(g)(f(v+g)\nabla f(v) - f(v)\nabla_g f(v+g))\, dg,$$

with $v + g \in \mathcal{B}(0, 3R)$.

Proof. Indeed, if v and $v + g \in \mathcal{B}(0, R)$ then

$$|g| = |v - v - g| \le |v| + |v + g| \le 2R.$$

Otherwise, if v or $v + g \notin \mathcal{B}(0, R)$ then

$$Q_L(f, f)(v) = 0.$$

Finally $v \le R$ and $g \le 2R$ implies

$$|v + g| \le |v| + |g| \le 3R.$$

■

Thus, as for the Boltzmann equation [25, 26], in order to develop a spectral approximation to (1.2) we can consider the distribution function $f(v)$ restricted on the cube $[-T, T]^3$ with $T \ge 3R$, assuming $f(v) = 0$ on $[-T, T]^3 \setminus \mathcal{B}(0, R)$, and extend it by periodicity to a periodic function on $[-T, T]^3$. As observed in [26], in practice, since f is assumed to be a periodic function, it is enough to take $T \ge 2R$ to prevent intersections of the regions where f is different from zero. To simplify the notation, from now on we will assume $T = \pi$ and hence $R = \pi/2$.

The distribution function f_N is approximated by the truncated Fourier series

$$f_N(v) = \sum_{k=-N}^{N} \hat{f}_k e^{ik\cdot v}, \tag{2.13}$$

$$\hat{f}_k = \frac{1}{(2\pi)^3} \int_{[-\pi,\pi]^3} f(v) e^{-ik\cdot v}\, dv. \tag{2.14}$$

Here we use a compact notation to denote the Fourier modes and its summation. By k we actually mean a vector with integer components, (k_1, k_2, k_3), and the summation of any quantity $h_k = h_{(k_1,k_2,k_3)}$ that depends on k is to be interpreted as

$$\sum_{k=-N}^{N} h_k \equiv \sum_{k_1=-N}^{N} \sum_{k_2=-N}^{N} \sum_{k_3=-N}^{N} h_{(k_1,k_2,k_3)}.$$

We obtain a set of ordinary differential equations for the coefficients $\hat{f}_k$ by requiring that the residual of (2.12) be orthogonal to all trigonometric polynomials of degree $\leq N$ [8, 17]. Hence for $k = -N, \ldots, N$

$$\int_{[-\pi,\pi]^3} \left(\frac{\partial f_N}{\partial t} - Q_L(f_N, f_N) \right) e^{-ik\cdot v}\, dv = 0. \tag{2.15}$$

By substituting expression (2.13) in (2.12) we get

$$Q_L(f_N, f_N) = \sum_{l=-N}^{N} \sum_{m=-N}^{N} \hat{f}_l \hat{f}_m \hat{\beta}_L(l,m)\, e^{i(l+m)\cdot v},$$

where

$$\hat{\beta}_L(l,m) = \int_{\mathcal{B}(0,\pi)} \Psi(g)[(l+m)(l-m) - (l+m)\cdot\mu(l-m)\cdot\mu]\, e^{ig\cdot m}\, dg,$$

with $\mu = g/|g|$. The previous expression can be rewritten, as in the Boltzmann case, as a difference of two terms, $\hat{\beta}_L(l,m) = \hat{B}_L(l,m) - \hat{B}_L(m,m)$, where the *FPL kernel modes* $\hat{B}_L(l,m)$ are given by

$$\hat{B}_L(l,m) = \int_{\mathcal{B}(0,\pi)} \Psi(g)[l^2 - (l\cdot\mu)^2] e^{ig\cdot m}\, dg. \tag{2.16}$$

It is very remarkable that (2.16) is a scalar quantity completely independent of the function f_N and of the argument v. In addition it can be easily proved that

PROPOSITION 2.2. *Let $\hat{B}_L(l,m)$ be defined by* (2.16). *Then*

(*i*) $\hat{B}_L(l,m) = \hat{B}_L(-l,m) = \overline{\hat{B}_L(l,-m)} = \hat{B}_L(l,-m)$.
(*ii*) $\hat{B}_L(m,m)$ *is a function of* $|m|$.
(*iii*) *If the kernel* $\Psi(g) = \Lambda|g|^{2+\gamma}$ *then* $|\hat{B}_L(l,m)| \leq |l|^2 \hat{B}_L(0,0)$, *where*

$$\hat{B}_L(0,0) = 4\pi \frac{\pi^{\gamma+5}}{\gamma+5}\Lambda.$$

Finally, using the orthogonality property we get from (2.15) the scheme

$$\frac{\partial \hat{f}_k}{\partial t} = \sum_{\substack{l+m=k \\ l,m=-N}}^{N} \hat{f}_l \hat{f}_m \hat{\beta}_L(l,m), \quad k = -N, \ldots, N. \tag{2.17}$$

Remark 2.1.

- As a consequence of point (*ii*) and of the fact that Ψ depends only on $|g|$, the Landau kernel modes are real.
- Scheme (2.17) has exactly the same structure of the Boltzmann scheme derived in [25, 26]. The only difference is the presence of the FPL kernel modes instead of the Boltzmann kernel modes.

2.2. *Main Properties*

Let us first set up the mathematical framework of our analysis. For any $t \geq 0$, $f_N(v,t)$ is a trigonometric polynomial of degree N in v; i.e., $f_N(t) \in \mathbb{P}^N$ where

$$\mathbb{P}^N = \text{span}\{e^{ik\cdot v} | -N \leq k_j \leq N,\ j = 1,2,3\}.$$

Moreover, let $\mathcal{P}_N : L^2([-\pi,\pi]^3) \to \mathbb{P}^N$ be the orthogonal projection upon $\mathbb{P}^N$ in the inner product of $L^2([-\pi,\pi]^3)$ (see (2.15)):

$$\langle f - \mathcal{P}_N f, \phi \rangle = 0, \quad \forall \phi \in \mathbb{P}^N.$$

We denote the L^2-norm by

$$\| f \|_2 = (\langle f,\ f \rangle)^{1/2}.$$

With this definition $\mathcal{P}_N f = f_N$, where f_N is the truncated Fourier series of f (2.13) and the method defined by (2.17) can be written in equivalent form as

$$\frac{\partial f_N}{\partial t} = Q_N^L(f_N,\ f_N) \tag{2.18}$$

with the initial condition

$$f_N(v, t=0) = f_{0,N}(v), \tag{2.19}$$

where we denote with $Q^L(f,\ f)$ the FPL collision operator with cutoff over the relative velocity and $Q_N^L(f,\ f) := \mathcal{P}_N Q^L(f_N,\ f_N)$. We point out that because of the periodicity assumption on f the collision operator $Q^L(f,\ f)$ preserves in time the mass contained in the period. In contrast, momentum and energy are not preserved in time.

From point (*i*) of Proposition 2.2 it is also clear that the projected collision operator $Q_N^L(f_N,\ f_N)$ will preserve the mass in time. In fact, from

$$\rho = \int_{[-\pi,\pi]^3} f_N(v)\, dv = (2\pi)^3 \hat{f}_0,$$

we obtain

$$\frac{d\hat{f}_0}{dt} = \sum_{m=-N}^{N} \hat{f}_{-m} \hat{f}_m (\hat{B}_L(-m,m) - \hat{B}_L(m,m)) = 0,$$

since $\hat{B}_L(-m,m) = \hat{B}_L(m,m)$.

Next if we denote by $H_p^r([-\pi,\pi]^3)$, where $r \geq 0$ is an integer, the subspace of the Sobolev space $H^r([-\pi,\pi]^3)$, which consists of periodic functions [8], we can state the following [29]:

PROPOSITION 2.3. *Let* $f, g \in L^2([-\pi,\pi]^3)$. *Then*

$$\|Q^L(f,g)\|_2 \le C\|g\|_1\|f\|_{H^2_p}.$$

Following the same strategy as in [26], we can show that consistency and spectral accuracy of the method will be a consequence of the previous estimate of the real FPL operator.

The consistency of the L^2 norm for the approximation of the FPL collision operator $Q^L(f,f)$ with $Q^L_N(f_N,f_N)$ is given by

THEOREM 2.1. *Let* $f \in H^2_p([-\pi,\pi]^3)$. *Then* $\forall r \ge 0$

$$\left\|Q^L(f,f) - Q^L_N(f_N,f_N)\right\|_2 \le C\left(\|f - f_N\|_{H^2_p} + \frac{\|Q^L(f_N,f_N)\|_{H^r_p}}{N^r}\right), \quad (2.20)$$

where C *depends on* $\|f\|_2$.

Proof. First, we can split the error into two parts:

$$\begin{aligned}&\left\|Q^L(f,f) - Q^L_N(f_N,f_N)\right\|_2\\ &\quad\le \|Q^L(f,f) - Q^L(f_N,f_N)\|_2 + \left\|Q^L(f_N,f_N) - Q^L_N(f_N,f_N)\right\|_2.\end{aligned}$$

Now clearly $Q^L(f_N,f_N) \in I\!P^{2N}$ and hence $Q^L(f_N,f_N)$ is periodic and infinitely smooth together with all its derivatives. Thus [8]

$$\left\|Q^L(f_N,f_N) - Q^L_N(f_N,f_N)\right\|_2 \le \frac{C}{N^r}\|Q^L(f_N,f_N)\|_{H^r_p}, \quad \forall r \ge 0. \quad (2.21)$$

Applying Proposition 2.3 and the identity

$$Q^L(f,f) - Q^L(g,g) = Q^L(f+g, f-g)$$

we have

$$\begin{aligned}&\|Q^L(f,f) - Q^L(f_N,f_N)\|_2\\ &\quad= \|Q^L(f+f_N, f-f_N)\|_2 \le C\|f+f_N\|_1\|f-f_N\|_{H^2_p} \le 2C_1\|f\|_2\|f-f_N\|_{H^2_p}.\end{aligned}$$

■

Finally the following corollary states the spectral accuracy of the approximation of the FPL collision operator:

COROLLARY 2.1. *Let* $f \in H^r_p([-\pi,\pi]^3)$, $r \ge 2$. *Then*

$$\left\|Q^L(f,f) - Q^L_N(f_N,f_N)\right\|_2 \le \frac{C}{N^{r-2}}\left(\|f\|_{H^r_p} + \|Q^L(f_N,f_N)\|_{H^r_p}\right). \quad (2.22)$$

Proof. It is enough to observe that

$$\|f - f_N\|_{H^2_p} \le \frac{C}{N^{r-2}}\|f\|_{H^r_p}.$$

■

Remark 2.2. From the previous corollary it follows that

$$\left|\langle Q^L(f,f),\varphi\rangle - \left\langle Q_N^L(f_N,f_N),\varphi\right\rangle\right| \le \frac{C}{N^{r-2}}\|\varphi\|_2\left(\|f\|_{H_p^r} + \|Q^L(f_N,f_N)\|_{H_p^r}\right),$$

and hence, by taking $\varphi = v, v^2$, the spectral accuracy of the moments. In particular it follows that, except for the projection errors on the initial data, the variations of momentum and energy introduced by the semidiscrete scheme are spectrally small and hence the observed variations with respect to the projected moments are due to the aliasing of periods. Aliasing effects are always present when one approximates a vanishing function by a periodic function (see [8, 17]).

3. AN $n \log_2 n$ EXACT ALGORITHM

Let us rewrite scheme (2.17) in the form

$$\frac{\partial \hat f_k}{\partial t} = \sum_{m=-N}^{N} \hat f_{k-m}\hat f_m \hat\beta_L(k-m,m), \quad k = -N,\dots,N. \tag{3.23}$$

In the previous expression we assume that the Fourier coefficients are extended to zero for $|k_j| > N$, $j = 1,2,3$. The straightforward evaluation of (3.23) requires exactly $O(n^2)$ operations, where $n = N^d$ and $d \ge 2$ is the dimension of the velocity space. As we will see, thanks to the particular structure of the kernel modes, using transform methods it is possible to reduce the computational cost to only $O(n\log_2 n)$ operations.

To this aim we observe that the term $\hat B_L(l,m)$ splits as

$$\begin{aligned}\hat B_L(l,m) &= l^2\int_{\mathcal{B}(0,\pi)} \Psi(g)e^{ig\cdot m}dg - \sum_{p,q=1}^{d} l_p l_q \int_{\mathcal{B}(0,\pi)} \Psi(g)\mu_p\mu_q e^{ig\cdot m}\,dg \\ &:= l^2F(m) - \sum_{p,q=1}^{d} l_p l_q I_{pq}(m) \\ &= l^2F(m) - l\,\mathcal{I}(m)\,l^T,\end{aligned} \tag{3.24}$$

where l^T denotes the transpose of the vector $l = (l_1,l_2,l_3)$ and $\mathcal{I} = (I_{pq})$ is a 3×3 symmetric matrix.

Thus we can write

$$\hat\beta_L(l,m) = l^2F(m) - l\,\mathcal{I}(m)l^T - \hat B_L(m,m), \tag{3.25}$$

and so the resulting scheme requires the evaluation of $d(d+1)/2+1$ convolution sums for the gain term (the number of distinct elements of $\mathcal{I}$ plus one) and a single convolution sum for the loss term:

$$\begin{aligned}\frac{\partial \hat f_k}{\partial t} &= \sum_{m=-N}^{N} \hat f_{k-m}\hat f_m (k-m)^2F(m) - \sum_{m=-N}^{N} \hat f_{k-m}\hat f_m \hat B_L(m,m) \\ &\quad - \sum_{p,q=1}^{d}\sum_{m=-N}^{N} \hat f_{k-m}\hat f_m (k_p-m_p)(k_q-m_q)I_{pq}(m).\end{aligned}$$

It is well-known that transform methods enable us to evaluate a convolution sum of the form

$$S(k) = \sum_{m=-N}^{N} f(k-m)g(m), \tag{3.26}$$

where f and g are arbitrary functions of $\mathbb{Z}^d$ in $\mathbb{R}$, in $O(n \log_2 n)$ operations instead of $O(n^2)$ [8]. This can be easily achieved in the following way:

- First, using the FFT algorithm one transforms f and g to $\hat{f}$ and $\hat{g}$ at a cost $O(n \log_2 n)$.
- Next one performs a term by term multiplication of the transformed functions $\hat{f}$ and $\hat{g}$ at a cost $O(n)$.
- Finally it is enough to transform the result through the inverse FFT algorithm at a cost $O(n \log_2 n)$ to determine $S(k)$.

For the details of the implementation of this standard technique for spectral methods we refer the reader to [8]. In a separate Appendix we give the details of the computation of $\hat{B}_L(l, m)$.

4. NUMERICAL TESTS

In this section we perform some numerical tests of the scheme, to check the spectral accuracy and the efficiency of the method.

4.1. *Time Discretization*

All calculations have been performed by a fourth-order Adams–Bashforth scheme, with fixed time step.

The first three values of the sequence have been computed by a fourth-order explicit Runge–Kutta scheme. This Adams–Bashforth scheme provides the high temporal accuracy needed to demonstrate spectral accuracy in velocity, at the cost of only one function evaluation per time step.

The FPL equation suffers from the stiffness typical of diffusion equations. The stability condition requires that the time step scales with the square of the velocity step. This means that by doubling the number of Fourier modes per direction, the total number of time steps becomes four times bigger to compute up to the same final time. We have not performed a stability analysis of the scheme, and the stability condition used in the computation has been found empirically.

No attempt has been made to overcome the numerical stiffness of the problem caused by diffusion. Although this is a very important issue and deserves a careful study, it is beyond the scope of the present paper. Further comments will be found in the last section.

4.2. *Test Cases*

We consider three test cases.

Test #1 (*BKW exact solution*)

Two dimensions in velocity space. Maxwellian molecules (i.e., $\gamma = 0$), with $C_0 = 1/(2\pi)$.

Initial condition:

$$f(v,0) = \frac{v^2}{\pi\sigma^2}\exp(-v^2/\sigma^2).$$

Integration time: $t_{\max} = 15$. This problem has an exact solution given by [4, 19]

$$f(v,t) = \frac{1}{2\pi S^2}\left(2S - 1 + \frac{1-S}{2S}\frac{v^2}{\sigma^2}\right)\exp\left(-\frac{v^2}{2S\sigma^2}\right),$$

where $S = 1 - \exp(-\sigma^2 t/8)/2$. In the computation, the scaling parameter σ is chosen in such a way that the numerical support of the initial condition is well approximated by $\mathcal{B}(0,\pi)$.

This test is used to check spectral accuracy, by comparing the error at a given time, when using $n = 8$, 16, 32, and 64 Fourier modes for each dimension.

Test #2 (*Sum of two Gaussians*)

Three dimensions in velocity space. Coulomb case (i.e., $\gamma = -3$), with $C_0 = 1/(4\pi)$.

Initial condition:

$$f(v,0) = \frac{1}{2(2\pi\sigma^2)^{3/2}}\left[\exp\left(-\frac{|v-2\sigma e_1|^2}{2\sigma^2}\right) + \exp\left(-\frac{|v+2\sigma e_1|^2}{2\sigma^2}\right)\right],$$

with $\sigma = \pi/10$. Integration time: $t_{\max} = 10$.

Here $e_1 \equiv (1,0,0)$ denotes the unit vector in the direction v_x.

This test is used to compute the evolution of the entropy and of the second-order moments.

Test #3 (*Rosenbluth problem*)

Three dimensions in velocity space. Coulomb case, with $C_0 = 1/(4\pi)$ as before.

Initial condition:

$$f(v,0) = \frac{1}{S^2}\exp\left(-S\frac{(|v|-\sigma)^2}{\sigma^2}\right),$$

with $\sigma = 0.3$ and $S = 10$.

Integration time: $t_{\max} = 900$.

This test is used to compute the evolution of the solution in time and to compare the results with those obtained in [6, 31].

4.3. *Numerical Results*

For the first test, we compute the error by comparing the numerical solution to the exact solution. In Table I we report the relative L^∞, L^1, and L^2 norms of the error at time $t = 1$ for $\sigma = \pi/V_{\max}$ and $V_{\max} = 6.6$. In the last three columns the order of accuracy is reported, computed as $\log_2(\mathrm{err}_i/\mathrm{err}_{i+1})$. The same quantities are reported in Table II when the solution is very close to equilibrium, at time $t = 100$ for $V_{\max} = 7.7$.

In Table III we report the corresponding error in energy, together with the velocity at which the maximum error occurs.

The relative norms of the error are computed as

$$\mathrm{err}_\infty(t) = \frac{\max_k|e_k(t)|}{\max_k|f(v_k,t)|}, \tag{4.27}$$

TABLE I
Short-Time Convergence Test for Maxwell Molecules in 2D

	Error at time $t = 1$ for $V_{\max} = 6.6$			Convergence rate		
# modes	L^∞	L^1	L^2	L^∞	L^1	L^2
8×8	1.68×10^{-1}	2.67×10^{-1}	1.39×10^{-1}	3.52	3.00	3.13
16×16	1.46×10^{-2}	3.32×10^{-2}	1.59×10^{-2}	12.98	13.46	13.35
32×32	1.80×10^{-6}	2.94×10^{-6}	1.52×10^{-6}	7.47	8.05	7.60
64×64	1.01×10^{-8}	1.11×10^{-8}	7.84×10^{-9}	—	—	—

$$\mathrm{err}_1(t) = \frac{\sum_k |e_k(t)|}{\sum_k |f(v_k, t)|}, \tag{4.28}$$

$$\mathrm{err}_2(t) = \left(\frac{\sum_k |e_k(t)|^2}{\sum_k |f(v_k, t)|^2} \right)^{1/2}, \tag{4.29}$$

where $f(v_k, t)$ is the exact solution, and $e_k(t) \equiv f(v_k, t) - f_N(v_k, t)$ is the difference between the exact and the numerical solution.

The rate at which the error decays with the increase of the number of modes is an indication of spectral accuracy. When the number of modes becomes higher, however, the order of accuracy does not increase. This is because the main cause of error is the approximation of the distribution function with a periodic function in phase space. In other words, the dominant error is aliasing error.

This effect is more evident by looking at the figures. In Fig. 1 for large time the aliasing error is dominant, and there is no gain in using a finer grid. In fact, when using more grid points, one should also increase the period, so that the discretization error is comparable with the aliasing error. In Fig. 2 the result of similar computation is shown, but a larger period has been used by taking $\sigma = \pi/7.7$. In this case the aliasing error is reduced and accuracy is greatly improved by increasing the number of Fourier modes. Clearly, for very long times the dominant error is again due to aliasing (see Table II). For a more detailed discussion of this issue see [26].

For the second test we compute the entropy decay (Fig. 3) and the evolution of the temperature T_x and T_y (Fig. 4) defined by

$$T_x = \frac{\int (v_x - u_x)^2 f(v)\, dv}{\int f(v)\, dv}, \quad T_y = \frac{\int (v_y - u_y)^2 f(v)\, dv}{\int f(v)\, dv},$$

TABLE II
Long-Time Convergence Test for Maxwell Molecules in 2D

	Error at time $t = 100$ for $V_{\max} = 7.7$			Convergence rate		
# modes	L^∞	L^1	L^2	L^∞	L^1	L^2
16×16	4.37×10^{-2}	2.98×10^{-2}	2.80×10^{-2}	12.31	11.93	12.20
32×32	8.63×10^{-6}	7.66×10^{-6}	5.96×10^{-6}	2.92	3.03	2.91
64×64	1.14×10^{-6}	9.37×10^{-7}	7.94×10^{-7}	—	—	—

TABLE III

Short- and Long-Time Behavior of the Relative Error in fv^2 for Maxwell Molecules in 2D

	$t = 1$, $V_{\max} = 6.6$		$t = 100$, $V_{\max} = 7.7$	
# modes	L^∞ error in fv^2	Position	L^∞ error in fv^2	Position
8×8	1.51×10^{-1}	$(-3.3, 3.3)$	—	—
16×16	9.92×10^{-2}	$(0.0, 6.6)$	4.71×10^{-2}	$(0.0, -7.7)$
32×32	1.41×10^{-4}	$(6.6, 0.0)$	2.22×10^{-5}	$(1.925, -0.9625)$
64×64	2.59×10^{-6}	$(0.0, -3.3)$	1.14×10^{-6}	$(-4.09, 1.925)$

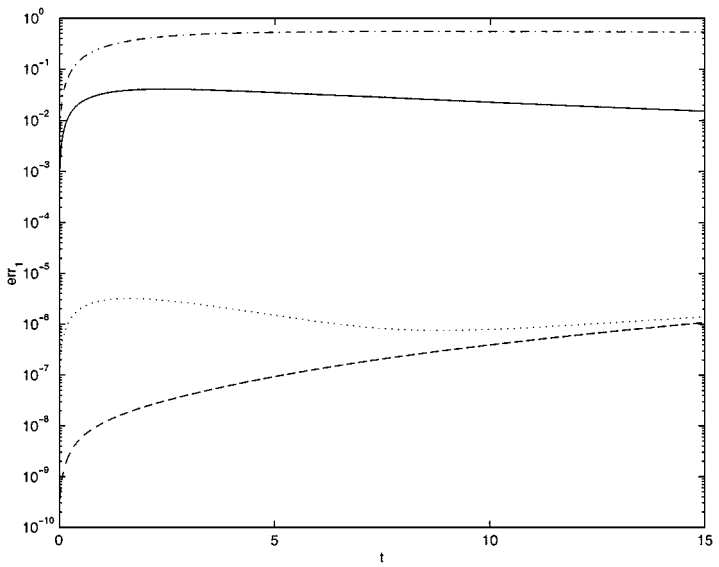

FIG. 1. Relative L^1 norm of the error for Test #1. $V_{\max} = 6.6$. Number of modes: 8^2 (dot–dashed line), 16^2 (continuous line), 32^2 (dotted line), 64^2 (dashed line).

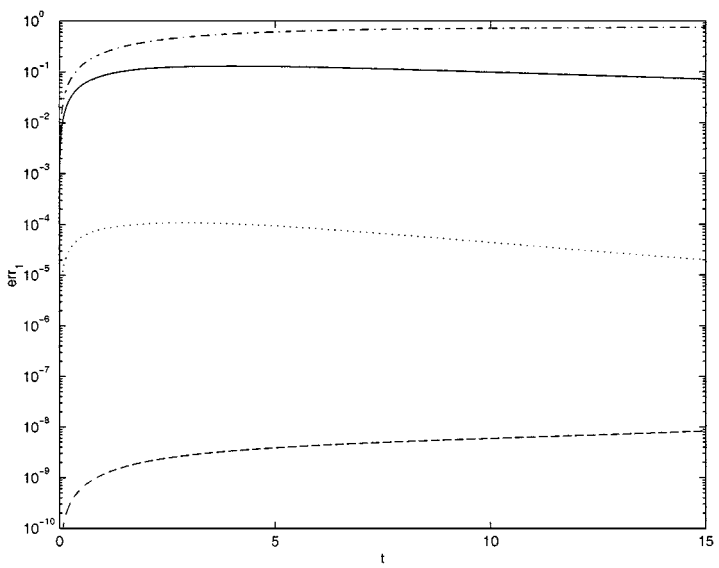

FIG. 2. Relative L^1 norm of the error for Test #1. $V_{\max} = 7.7$. Number of modes: 8^2 (dot–dashed line), 16^2 (continuous line), 32^2 (dotted line), 64^2 (dashed line).

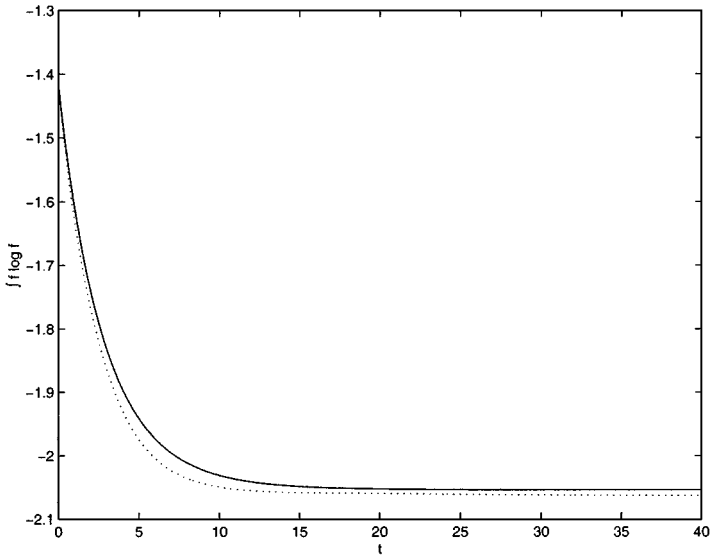

FIG. 3. Entropy decay for Test #2. Number of modes: 16^3 (dotted line) and 32^3 (continuous line).

where u_x and u_y are the components of the mean velocity. In the figures, the dotted line is obtained with 16^3 modes and the continuous line with 32^3 modes. The entropy is computed by discretizing the expression

$$H = \int_{[-T,T]^3} f(v) \log f(v)\, dv$$

on the velocity grid by a straightforward formula.

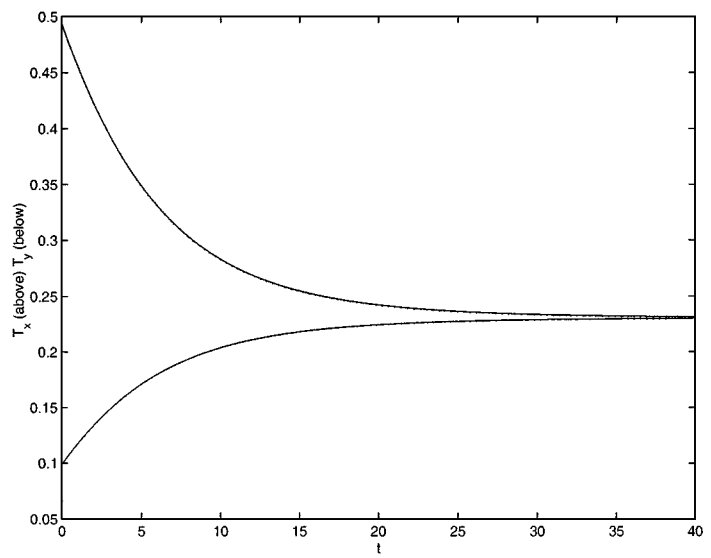

FIG. 4. Temperature evolution for Test #2. Number of modes: 16^3 (dotted line) and 32^3 (continuous line).

TABLE IV
Computational Costs (Seconds) for One Evaluation of the FPL Operator in 2D and 3D

2D		3D	
# modes	CPU time	# modes	CPU time
8×8	0.0055	$8 \times 8 \times 8$	0.20
16×16	0.027	$16 \times 16 \times 16$	2.15
32×32	0.16	$32 \times 32 \times 32$	23.3
64×64	0.73	—	—

The computation times for the evaluation of the collision operator are reported in Table IV. All the calculations, including the tests for the computation time, have been performed on a simple Intel Pentium 266 MHz machine, running under Linux. Note that the increase of the computational time is in good agreement with the theoretical prediction, since it increases approximatively as $n \log_2 n$.

For the last test case we compute the time evolution of the distribution function.

In Figs. 5 and 6 computations performed respectively with $N = 16^3$ and $N = 32^3$ modes are reported. In the figures we show the cross section of the distribution function at times $t = 0, 9, 36, 81, 144, 225$, and 900. The results are in good agreement with those presented in [6, 31].

5. FUTURE DEVELOPMENTS

We have presented a way to construct fast spectral methods for the FPL equation.

The present work is a first step in the construction of an effective scheme for the numerical solution of the FPL equation. The method should be suitable for treating cases where the

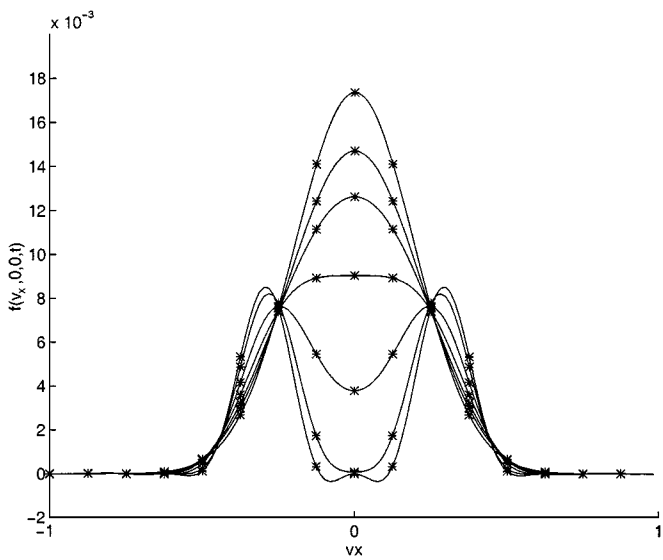

FIG. 5. Cross section of the distribution function at different times, for Test #3. Number of modes: 16^3. Grid values ($*$); trigonometric reconstruction (continuous line).

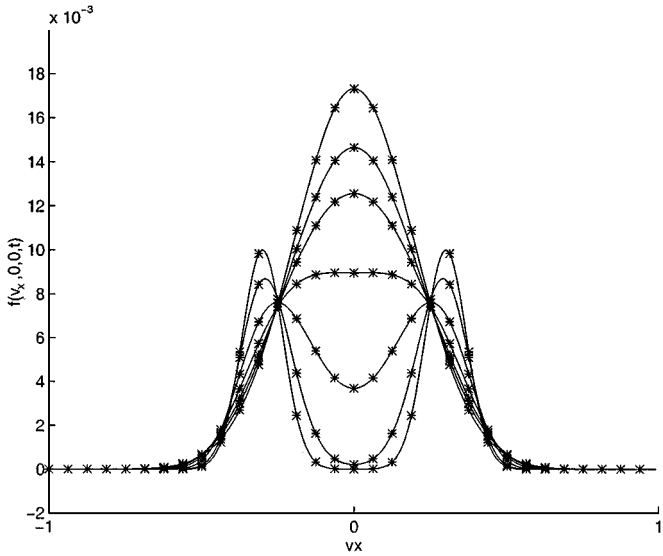

FIG. 6. Cross section of the distribution function at different times, for Test #3. Number of modes: 32^3. Grid values ($*$); trigonometric reconstruction (continuous line).

distribution function can be effectively described with a reasonably low number of Fourier modes. This is the case, in particular, of smooth distribution functions.

The main features of the method are its simplicity and generality and the possibility of providing spectrally accurate numerical approximations with a strong reduction in the computational cost. In fact, using transform methods it is possible to evaluate exactly the spectral scheme with only $O(n \log_2 n)$ operations as opposed to the usual $O(n^2)$ cost. From a physical point of view the method preserves the mass whereas the other physical properties, such as conservation of momentum and energy are "spectrally preserved." These properties are strongly influenced by the aliasing effects in the scheme and hence depend on the choice of the computational domain in the velocity space.

The problem of finding a suitable time discretization to avoid the restriction on the time step needs further investigations. This problem has been treated with implicit schemes in [9, 20] for the Fokker–Planck equation and in [15] for the FPL equation in the radially symmetric case.

For the general case this problem is not easy to solve, and the use of implicit schemes would be very expensive. An alternative to an implicit scheme could be the use of explicit schemes with a large stability region [22]. Such an approach is under investigation [24].

In the near future we plan to extend this approach to spatially nonhomogeneous situations.

APPENDIX

Computation of the Kernel Modes

We will restrict ourselves here to the case of inverse-power laws; hence $\Psi(g) = \Lambda |g|^{\gamma+2}$. To simplify notation we fix $\Lambda = 1$.

To implement the scheme, the following quantities are needed:

$$F(m) = \int_{\mathcal{B}(0,\pi)} |g|^{2+\gamma} e^{ig\cdot m}\, dg$$

and

$$I_{pq}(m) = \int_{\mathcal{B}(0,\pi)} |g|^{\gamma} g_p g_q e^{ig\cdot m}\, dg, \quad p, q = 1, \dots, d.$$

We consider separately the computation of the coefficients in 2D and 3D.

2D Case

A simple calculation (see [26]) shows that in two dimensions

$$\tilde{F}(m) = F(|m|) = 2\pi \int_0^{\pi} r^{\gamma+3} J_0(|m|r)\, dr, \tag{A.30}$$

where J_0 is the Bessel function of order 0.

In addition it can be shown that

$$\begin{aligned} I_{11}(m) &= \frac{1}{2}\left[F(|m|) + \frac{m_1^2 - m_2^2}{|m|^2} G(|m|)\right], \\ I_{22}(m) &= \frac{1}{2}\left[F(|m|) - \frac{m_1^2 - m_2^2}{|m|^2} G(|m|)\right], \\ I_{12}(m) &= I_{21}(m) = \frac{m_1 m_2}{|m|^2} G(|m|), \end{aligned} \tag{A.31}$$

where

$$G(|m|) = \int_0^{\pi} r^{\gamma+3} C(|m|r)\, dr \tag{A.32}$$

and

$$C(x) = \int_0^{2\pi} \cos(x\cos\phi)\cos(2\phi)\, d\phi. \tag{A.33}$$

Thus the computation of the FPL kernel modes in 2D reduces simply to the computation of two one-dimensional integrals $F(|m|)$ and $G(|m|)$ for each m. These quantities can be computed very accurately once and then stored in two bidimensional arrays.

A very efficient way to compute all these integrals in $O(N^2)$ operations is the following. First write the integral F as

$$F(|m|) = \frac{2\pi}{|m|^{\gamma+4}} F_1(\pi|m|) \tag{A.34}$$

with

$$F_1(z) = \int_0^{z} x^{\gamma+3} J_0(x)\, dx.$$

Because the coefficients depend only on $|m|$, it is enough to compute them for $m = (m_1, m_2)$, with $0 \le m_1 \le m_2 \le N$. Let us sort those points in increasing size: $m^{(j)}$, $j = 1, \ldots, (N+1)(N+2)/2$, $|m^{(j+1)}| \ge |m^{(j)}|$. Then one is left with the computation of $F(\pi|m^{(j)}|)$. This computation involves the evaluations of integrals of the form

$$\int_{\pi|m^{(j)}|}^{\pi|m^{(j+1)}|} x^{\gamma+3} J_0(x)\, dx.$$

Note that many such integrals are zero—those for which $|m^{(j)}| = |m^{(j+1)}|$. Furthermore, the integration interval is very small; therefore the integrals are accurately computed with few calculations. Because the function is regular, we used an adaptive Romberg quadrature rule, with tolerance 10^{-13}.

The value of

$$F(0) = 2\pi \frac{\pi^{\gamma+4}}{\gamma+4}$$

is computed analytically.

For the computation of $G(|m|)$, we use the same technique, giving

$$G(|m|) = \frac{1}{|m|^{\gamma+4}} F_2(\pi|m|),$$

where

$$F_2(z) = \int_0^z x^{\gamma+3} C(x)\, dx.$$

The function F_2 can be computed on the grid by using the same technique used for the computation of $F_1(x)$. The function $C(x)$ is computed by cubic spline interpolation of precomputed values of the integral (A.33) on a uniform grid in the interval $[0, R_{\max}]$, with $R_{\max} = N\pi\sqrt{2}$. The number of grid points for the computation of C has been chosen as $N_p = [20R_{\max}]$ ($[\cdot]$ denotes the integer part). The computation of the values of $C(x)$ on a grid is performed by simple trapezoidal rule, which is spectrally accurate in this case, since the integrand is periodic. The values of the derivative of $C(x)$ at the extrema are precomputed and used to determine the coefficients of the spline interpolation.

3D Case

It is easy to verify that (see [26]) in three dimensions

$$\tilde{F}(m) = F(|m|) = \frac{4\pi}{|m|^{\gamma+5}} F_3(\pi|m|), \tag{A.35}$$

where

$$F_3(z) = \int_0^z x^{\gamma+3} \sin(x)\, dx.$$

The function $F_3(\pi|m|)$ can be efficiently computed on the three-dimensional grid $m = (m_1, m_2, m_3)$, $0 \le m_1 \le m_2 \le m_3$, by using the same technique used in the computation

of $F_1(z)$. The value for $m = 0$ is computed analytically and is

$$F(0) = 4\pi \frac{\pi^{\gamma+5}}{\gamma+5}.$$

The computation of $I_{\alpha\beta}$ is a little more involved. Let us start from the definition

$$I_{\alpha\beta}(m) = \int_{B(0,\pi)} |q|^\gamma \exp(iq \cdot m) q_\alpha q_\beta \, dq.$$

Because of the symmetries of $\mathcal{I}$, it is enough to compute $I_{33}(m)$ and $I_{12}(m)$, for $m = (m_1, m_2, m_3)$, with $0 \le m_1 \le m_2 \le N$, $0 \le m_3 \le N$. We have

$$\begin{aligned}
I_{33}(m_2, m_1, m_3) &= I_{33}(m_1, m_2, m_3),\\
I_{33}(-m_1, m_2, m_3) &= I_{33}(m_1, m_2, m_3),\\
I_{33}(m_1, m_2, -m_3) &= I_{33}(m_1, m_2, m_3),\\
I_{12}(m_2, m_1, m_3) &= I_{12}(m_1, m_2, m_3),\\
I_{12}(-m_1, m_2, m_3) &= -I_{12}(m_1, m_2, m_3),\\
I_{12}(m_2, m_1, -m_3) &= I_{12}(m_1, m_2, m_3),\\
I_{11}(m_1, m_2, m_3) &= I_{33}(m_2, m_3, m_1),\\
I_{22}(m_1, m_2, m_3) &= I_{33}(m_3, m_1, m_2),\\
I_{23}(m_1, m_2, m_3) &= I_{12}(m_2, m_3, m_1),\\
I_{31}(m_1, m_2, m_3) &= I_{12}(m_3, m_1, m_2).
\end{aligned}$$

Evaluation of I_{33}

Simple computations show that

$$I_{33}(m_1, m_2, m_3) = 2\pi \int_0^\pi \rho^{\gamma+4} F_4\left(\rho m_3, \rho\sqrt{m_1^2 + m_2^2}\right) d\rho,$$

where

$$F_4(a, b) = \int_0^\pi \cos(a\cos\theta)\cos^2\theta \sin\theta J_0(b\sin\theta)\, d\theta.$$

Therefore

$$I_{33}(0) = \frac{4}{3}\frac{\pi^{\gamma+6}}{\gamma+5}.$$

For each value of m, I_{33} can be computed by a nested call of an adaptive quadrature routine. Note that the tolerance of the innermost quadrature call must be more stringent than the one of the outermost quadrature, in order to ensure convergence of the procedure.

Evaluation of I_{12}

Similarly to the previous case we have

$$I_{12}(m_1, m_2, m_3) = \frac{m_1 m_2}{m_1^2 + m_2^2} \int_0^\pi \rho^{\gamma+4} F_5\left(\rho m_3, \rho\sqrt{m_1^2 + m_2^2}\right) d\rho,$$

where

$$F_5(a, b) = \int_0^\pi \cos(a\cos\theta)\sin^3\theta C(b\sin\theta)\, d\theta$$

and $C(x)$ is defined in Eq. (A.33). Thus $I_{12}(0) = 0$, because $C(0) = 0$. As in the case of I_{33}, for each value of m, I_{12} can be computed by a nested call of an adaptive quadrature routine.

REFERENCES

1. A. A. Arsen'ev and O. E. Buryak, On the connection between a solution of the Boltzmann equation and a solution of the Fokker–Planck–Landau equation, *Math. USSR Sb.* **69**, 465 (1991).
2. Yu. A. Berezin, V. N. Khudick, and M. S. Pekker, Conservative finite difference schemes for the Fokker–Planck equation not violating the law of an increasing entropy, *J. Comput. Phys.* **69**, 163 (1987).
3. A. V. Bobylev, I. F. Potapenko, and V. A. Chuyanov, Completely conservative difference schemes for nonlinear kinetic equation of Landau (Fokker–Planck) type (in Russian), *Akad. Nauk SSSR Inst. Prikl. Mat. Preprint* **76**, 26 pp. (1980).
4. A. V. Bobylev and V. V. Vedenyapin, The Fourier transform of Boltzmann and Landau collision integrals (in Russian), *Akad. Nauk SSSR Inst. Prikl. Mat. Preprint* **125**, 16 (1981).
5. C. Buet and S. Cordier, Numerical analysis of conservative and entropy schemes for the Fokker–Planck–Landau equation, *SIAM J. Numer. Anal.* **36**, 953 (1999).
6. C. Buet and S. Cordier, Conservative and entropy decaying numerical scheme for the isotropic Fokker–Planck–Landau equation, *J. Comput. Phys.* **145**(1), 228 (1998).
7. C. Buet, S. Cordier, P. Degond, and M. Lemou, Fast algorithms for numerical, conservative, and entropy approximations of the Fokker–Planck equation, *J. Comput. Phys.* **133**, 310 (1997).
8. C. Canuto, M. Y. Hussaini, A. Quarteroni, and T. A. Zang, *Spectral Methods in Fluid Dynamics* (Springer-Verlag, New York, 1988).
9. J. S. Chang and G. Cooper, A practical difference scheme for Fokker–Planck equations, *J. Comput. Phys.* **6**, 1 (1970).
10. P. Degond and B. Lucquin-Desreux, The Fokker–Planck asymptotics of the Boltzmann collision operator in the Coulomb case, M^{3}AS **2**, 167 (1992).
11. P. Degond and B. Lucquin-Desreux, An entropy scheme for the Fokker–Planck collision operator of plasma kinetic theory, *Numer. Math.* **68**, 239 (1994).
12. L. Desvillettes, On asymptotics of the Boltzmann equation when the collisions become grazing, *Transp. Theory Stat. Phys.* **21**, 259 (1992).
13. L. Desvillettes and C. Villani, On the spatially homogeneous Landau equation for hard potentials. Part I: Existence, uniqueness and smoothness; Part II: H-theorem and applications, *Communications in PDEs* **25**, 179 (2000).
14. Yu. N. Dnestrovsij and D. P. Kostomarov, *Numerical Simulations of Plasmas* (Springer-Verlag, New York, 1986).
15. E. M. Epperlein, Implicit and conservative difference schemes for the Fokker–Planck equation, *J. Comput. Phys.* **112**, 291 (1994).
16. F. Filbet, in preparation.

17. D. Gottlieb and S. A. Orszag, *Numerical Analysis of Spectral Methods: Theory and Applications*, SIAM CBMS-NSF Series (Soc. for Industr. & Appl. Math, Philadelphia, 1977).
18. L. D. Landau, Die kinetische gleichung für den fall Coulombscher vechselwirkung, *Phys. Z. Sowjet.* **154** (1936); transl. as the transport equation in the case of the Coulomb interaction, in *Collected Papers of L. D. Landu*, edited by D. ter Haar (Pergamon, Oxford, 1981), p. 163.
19. M. Lemou, Multipole expansions for the Fokker–Planck–Landau operator, *Numer. Math.* **78**, 597 (1998).
20. E. W. Larsen, C. D. Levermore, G. C. Pomraning, and J. G. Sanderson, Discretization methods for one dimensional Fokker–Planck operators, *J. Comput. Phys.* **61**, 359 (1985).
21. B. Lucquin-Desreux, Discrétization de l'opérateur de Fokker–Planck dans le cas homogène, *C. R. Acad. Sci. Paris, Ser. 1* **A 314**, 407 (1992).
22. A. A. Medovikov, High order explicit methods for parabolic equations, *BIT* **38**(2), 372 (1998).
23. T. Ohwada, Higher order approximation methods for the Boltzmann equation, *J. Comput. Phys.* **139**, 1 (1998).
24. L. Pareschi and F. Filbet, in preparation.
25. L. Pareschi and B. Perthame, A Fourier spectral method for homogeneous Boltzmann equations, *Transp. Theory Stat. Phys.* **25**, 369 (1996).
26. L. Pareschi and G. Russo, Numerical solution of the Boltzmann equation I: Spectrally accurate approximation of the collision operator, *SIAM J. Numer. Anal.* **37**, 1217 (2000).
27. L. Pareschi and G. Russo, On the stability of spectral methods for the homogeneous Boltzmann equation, *Transp. Theory Stat. Phys.* **29** (2000).
28. L. Pareschi, G. Russo, and G. Toscani, Méthode spéctrale rapide pour l'equation de Fokker–Planck–Landau, *C. R. Acad. Sci. Paris, Ser. 1* **330**, 517 (2000).
29. L. Pareschi, G.Toscani, and C. Villani, Spectral methods for the non cut-off Boltzmann equation and numerical grazing collision limit, preprint (1999).
30. I. F. Potapenko and C. A. de Arzevedo, The completely conservative difference schemes for the nonlinear Landau–Fokker–Planck equation, *J. Comput. Appl. Math.* **103**, 115 (1999).
31. M. N. Rosenbluth, W. MacDonald, and D. L. Judd, Fokker–Planck equation for an inverse square force, *Phys. Rev.* **107**, 1 (1957).
32. G. Strang, On the construction and comparison of difference schemes, *SIAM J. Numer. Anal.* **5**, 506 (1968).
33. C. Villani, On a new class of weak solutions to the spatially homogeneous Boltzmann and Landau equations, *Arch. Rat. Mech. Anal.* **143**(3), 273 (1998).
34. F. S. Zaitsev, V. V. Longinov, M. R. O'Brien, and R. Tunner, Difference schemes for the time evolution of three-dimensional kinetic equations, *J. Comput. Phys.* **147**, 239 (1998).